OUTGASSING TESTS ON GRAPHITES IN THE TEMPERATURE RANGE 100-1600 °C

C. Alessandrini, M.L. Apicella, L. Verdini

Associazione EURATOM-ENEA sulla Fusione, C.R.E. Frascati,
P.O. Box 65 - 00044 Frascati, (Rome) (Italy)

ABSTRACT

Graphite is a an interesting material for plasma-facing components in fusion experiments, mainly because of its low atomic number and its excellent thermal properties. Nevertheless, it contains a large amount of gaseous impurities, which can be released by plasma-surface interaction and affect the purity of the deuterium-tritium plasma. To investigate the outgassing behaviour of graphites, CFCs and doped C composites, a facility has been set up to perform outgassing tests on samples (dim. 2x2x0.5 cm), as a function of temperature in the range between 100 and 1600°C. The experimental apparatus, designed to work in UHV conditions, allows outgassing measurements by a quadrupole mass spectrometer (1-200 AMU), using two different methods. The test facility, the quadrupole calibration and preliminary quantitative outgassing measurements on SEP CARB N112 samples are described.

1. Introduction

In the framework of the European Fusion Technology Programme, the Fusion Technology Division of ENEA has been assigned with the task of performing outgassing tests on candidate materials for the NET plasma-facing components.

In detail, the work consists in evaluating the outgassing behaviour of samples made of graphites, CFCs and doped C composites, by measuring the outgassing rate of H_2, H_2O, O_2, CO, CO_2 and CxHy species, as a function of temperature in the range 100:1600 °C and of pre-treatments.

An ad hoc facility has been built to measure the outgassing rate of samples (dim2×2×0.5 cm). The measuring apparatus, designed to work in UHV conditions, allows outgassing measurements by means of a quadrupole mass spectrometer (1-200 AMU) in two different ways:

a) pressure rise method;

b) known conductance method.

In the first method, the outgassing rate is measured by recording the increase of the total and partial pressures immediately after exclusion of the pumping system.

In the second, the measuring chamber is dynamically pumped through a (9.25 l/s for nitrogen) known conductance.

The outgassing rate is calculated by measuring the total and partial pressures and taking into account the effective pumping speed for each gas in the chamber.

The sample is heated up to 1600°C, using a RF inductive system. This technique was chosen to avoid heating other components in the vacuum chamber. To keep the outgassing noise level of the measuring chamber low and constant, the samples are inserted under vacuum by a load lock device.

2. Description of the test facility

The test facility (see Fig. 1) consists of a stainless steel measuring chamber, 30 cm in diameter, and 40 cm high, capable of reaching a base pressure in the range of 10^{-9} mbar, since it is pumped by a 500 l/s turbomolecular pump.

The measuring chamber is connected to the turbo through two vacuum lines, each with its gate valve, one (15 cm diam.) serving as the main pumping connection, the other (10 cm diam.) with the insertion of a 10-mm-diam. diaphragm used as by-pass for known conductance measurements. The sample is supported in the measuring chamber by a fork consisting of two parallel 1.5-mm-diam. tungsten wires inserted in two holes made in the sample.

Due to the reactions expected between graphite and refractory metals at high temperatures and in order to enable the extraction of the sample from its support, the contact between the sample and the tungsten wires is not direct but via intermediate tantalum tubes placed in the holes of the sample.

The facility is provided with a load lock chamber and a transfer system for inserting or extracting the sample under vacuum. The load lock chamber, connected to the measuring chamber through a 100 CF gate valve, consists of a 100 CF, six-way commercial cross pumped by a 110 l/s turbomelecular pump.

The transfer system consists of pliers shaped to accomodate the sample, which can be grasped or released thanks to two cams driven by a rotary feedthrough. The pliers are mounted on one end of a rod, which is able to move (450 mm stroke) from the load lock chamber to the measuring chamber by means of a rack and pignon device driven by a second rotary feedthrough. All the moving parts of the system are metallic and are lubricant-free since they are supported by ball bearings. The device allows highly precise and reproducible positioning of the sample (errors within 1/10 of mm). The inductive method was chosen to a heat the sample with a 22 kW, 500 KHz power supply providing 12 kW of RF power at the coil.

The coil consists of four turns of 5-mm-diam., 1-mm-thick copper tubing with an internal coil diameter of 30 mm. The coil is water cooled and connected to two electrical feedthroughs sealed on an alumina disc by means of viton "o" rings. Their utilization was invevitable, since any of the commercial ceramic-metal feedthroughs welded on a metallic flange would give rise to the RF heating effect of the metal between the two conductors.

The sample temperature is measured from 100°C to 1600°C through two sapphire windows, by two infrared pyrometers. To cover the whole temperature range, it was necessary to install two different pyrometers, one for 100 to 550°C, the other for 500 to 1600°C. The pyrometers are connected to the temperature control system, which automatically switches from one pyrometer to the other when the first approaches to its full scale and vice versa.

The programmable temperature control system connected to the RF power supply provides feedback control of the temperature and allows programming of up to ten temperature steps.

The facility is equipped with three ionization gauges, a quadrupole mass spectrometer and a capacitance manometer (MKS BARATRON, range 1-10^{-5} Torr).

The quadrupole control unit is interfaced with a computer for the acquisition of the measurements.

The facility is also provided with a gas inlet system for quadrupole calibration, which is performed by introducing known gases into the measuring chamber at known pressure (10^{-5} to 10^{-7} mbar) and recording the quadrupole mass spectrometer signal.

Since it is difficult to measure the low absolute pressure in the chamber, it is calculated using the capacitance manometer (Fig. 1, item B) to measure the relatively high pressure (10^{-2}:10^{-4} mbar) of gases charged in the small known volume (Fig. 1, item C) before letting them expand in the measuring chamber.

The gas inlet system has four bottles of different gases (H_2, CH_4, N_2, Ar) and all the necessary valves.

All the facility components, including all gate valves, exposed to vacuum are metal sealed and can be baked up to 300:400°C, with the exception of the electrical feedthroughs of the coil, which have viton "o" rings and can be baked to 200°C only.

3. Samples and their pre-treatment

Four parallelepiped-shaped samples (2×2×0.5 cm) were machined from a block of SEP CARB N112, and two small tantalum tubes inserted in each sample as described in Sec. 2.

The samples were then marked and cleaned and their whole surface polished with abrasive paper. Both during and after cleaning, gloves or pliers were used to handle the samples.

Sample No. 1 was tested without any heating pre-treatment, samples 2, 3 and 4 were pre-treated in a vacuum furnace at 1000°C for 20 h.

Samples 1 and 2 were weighed by a METLER micro balance with a sensitivity of 10^{-6} g; the first after cleaning, the second after cleaning and heating pre-treatment.

The net weights (subtracting the tantalum tubes) are: Sample No. 1: 3.606648 g; Sample No. 2: 3.632600 g.

4 . Quadrupole calibration

Calibration of the quadrupole is required to obtain quantitative partial pressure measurements. The aim of the calibration is to determine the experimental sensitivity factor of the instrument, defined as the ratio of the quadrupole current signal Ix (the highest ion peak) of the gas x to the pressure Px of the same gas:

$$Sx = Ix/Px.$$

Calibration tests were performed using both the static and the dynamic method utilizing four different gases (H_2, CH_4, N_2, Ar) at a pressure of 4×10^{-7}-4×10^{-5} mbar.

In the static method, a known amount of the calibration gas was introduced in the measuring chamber after closing the pumping system. The amount of gas had been pre-determined by filling a small known volume and measuring its pressure with a capacitance manometer before pouring the gas into the measurement chamber. The absolute pressure in the measuring chamber was calculated according to the following formula:

$$Pc = Pv \cdot V1 / (V1 + V2) = Pv/788 ,$$

where:

Pc = absolute pressure of the calibration gas in the measuring chamber (mbar),
Pv = absolute pressure in the small known volume (mbar),
V1 = 55 small known volume (cm^3),
V2 = 43300 volume of the measuring chamber (cm^3).

At each constant pressure in the chamber, the quadrupole current signal and ionization pressure were recorded.

The calibration tests based on this method were repeated several times. From the results we observe the following characteristics:

a) the dispersion of the results is so high that it is not possible to establish with sufficient certainty the trend of the sensitivity as a function of the pressure;

b) the sensitivity level of the quadrupole decreased constantly between one run of tests and the a subsequent run;

c) It takes such as a long time (at least one working day) to perform a complete run of tests that it was very difficult to make a sufficiently high number of tests for a statistical basis.

The second method consisted in introducing the calibration gas through a metering valve into the continuously pumped measuring chamber.

The quadrupole current signal was recorded at each constant pressure measured in the chamber by an ionization gauge, which was previously calibrated for each gas, exploiting the relation between the absolute pressure evaluated with the capacitance manometer and the pressure measured with the ionization gauge (see Fig. 2). For each gas, ten pressure-quadrupole signal series of measurements were performed in the range of $4\times10^{-8}\times4\times10^{-5}$ mbar.

This method compared with the static method has the following characteristics:

d) the tests can be done more quickly, so it was possible to make a large number of measurements for a wider statistical basis;

e) the measurements obtained have a lower dispersion of results (within ±30%);

f) the sensitivity level found with this method is lower.

The quicker method of testing, which allowed seven complete runs of measurements for each gas in a reasonable time, and the lower dispersion of results made it possible to find, with a better accuracy, a sensitivity-pressure dependence trend for each gas.

Dynamic calibration curves of the average sensitivity as a function of the pressure are reported in Figs 3,4,5,6 together with the limits of the maximum dispersion of the results.

Considering the difference in the sensitivity level between the two methods and that the outgassing measurements were performed using the static method, the sensitivity level of the static calibration was taken into account together with the trend of the reference dynamic calibration in order to interpret the results.

The static calibration sensitivity considered was that relative to the last calibration performed just before an outgassing test of a sample.

The sensitivity curve used to calculate the partial pressure was derived from the reference dynamic calibration curve corrected by a factor equal to the ratio between the average sensitivity levels of the two methods.

The conversion from the quadrupole signal to partial pressure is direct for those gases for which the calibration has been performed; for the other gases, sensitivity curves are calculated assuming as reference the available experimental curve of the gas with the closest mass and considering the following three parameters: fragmentation factor, ionization probability and transmission factor.

To obtain the calculated sensitivity curves, the following relations were used:

$$Sx = K \cdot Sy$$

$$K = (Fx/Fy)(\sigma x/\sigma y)(Tx/Ty)$$

$$Tx/Ty = My/Mx$$

where:

Sx = sensitivity of the gas x to be calculated;

Sy = sensitivity of the reference gas y with the closest mass to that of the gas x;

Fx = fragmentation factor of the gas x ;

Fy = fragmentation factor of the reference gas y ;

σx = relative ionization probability factor of the gas x respect to N_2;

σy = relative ionization probability factor of the reference gas y respect to N_2;

Tx = transmission factor of the gas x;

Ty = transmission factor of the reference gas y;

Mx =mass of the gas x;

My = mass of the reference gas y;

The fragmentation, relative ionization probability and transmission factors have been taken from the "Inficon Quadrex 200" residual gas analyser technical manual /1/.

In Figs 7 and 8 sensitivity curves as a function of the pressure are shown for the gases of interest. For a quicker conversion, curves of the quadrupole current signal as a function of the partial pressure have been plotted, as shown in Figs. 9 and 10.

5. Outgassing tests

Before starting outgassing measurements of the samples, a characterization of the measuring chamber was performed by measuring its outgassing rate to get the background level. Since the measuring chamber is heated by the sample radiation, its background was measured at different temperatures. At the maximum temperature of the sample (1600°C), the temperature measured on the chamber walls was 80 °C .

Figures 11,12 and 13 report the chamber temperature as a function of the sample temperature, the background as a function of the chamber temperature and the background as a function of the sample temperature, respectively.

Outgassing tests were made according to the original measuring programme, which includes tests of the samples in the following conditions:

a) without pre-treatment (as received);

b) after pre-treatment in a vacuum furnace at 1000 °C for 20 h and short exposure to air (about 2 h);

c) after pre-treatment and long exposure to air (about 2 months);

d) after pre-treatment and exposure to steam.

The outgassing measurements of two samples, Nos. 1 and 2, tested under conditions a) and b), respectively, are reported here. The tests relative to c) conditions, will be carried out in the near future, those relative to d) conditions will be performed grouping all the samples in a unique campaign after all other tests under conditions a), b) and c) have been completed.

The outgassing measurement tests were done at each constant temperature step, closing the pumping system and simultaneously recording the quadrupole current signal and total pressure rise as a function of time.

The samples were heated in steps of 200 °C with a temperature ramp of 100 °C per minute.

Sample No. 1 was tested up to only 600°C because its too high outgassing rate increased the pressure to the quadrupole operating limit.

The quadrupole current rate is calculated from the derivative of the quadrupole current signal as a function of time, and then converted into partial pressure rates, according to sec. 4.

The outgassing rates are calculated multiplying the partial pressure rates by the measuring chamber volume.

Figures 14 and 15 show outgassing rates of samples 1 and 2 for the most abundant gaseous species. The values are net since the background corresponding to the temperature of the chamber has been subtracted.

The most abundant gaseous species measured, amounting to about 90% of the total, were H_2, CH_4, H_2O, CO.

After the tests, the samples were weighed again, giving: sample No. 1: 3.602130 g; sample No. 2: 3.631090 g.

The differences of the weights before and after the tests are: sample No. 1 - 0.004518 g; sample No. 2 - 0.001510 g.

The loss of weight may depend on the outgassing effect, but a doubt exists that it could be caused by the abrasive action of the transfer system pliers, and further investigation is necessary.

6. Conclusions

The experience gained in carrying out the preliminary tests presented in this paper has shown the limits in reproducibility of the results of the static method. In fact, when the sample temperature increases following a temperature ramp the outgassing rate also increases. Once the pre-programmed temperature has been reached, the outgassing rate initially shows a maximum peak and afterwards exponentially decreases, even if the sample temperature remains constant.

The difference between the maximum peak value and the stabilized value may reach a decade of pressure.

As a consequence, the measured outgassing rate depends on the time elapsed between reaching the stable temperature and doing the test.

On the other hand, waiting for a stable pressure means measuring a lower outgassing rate than that corresponding to the maximum value.

Since the test requires several manual operations, there is uncertainty in the time reproducibility, which influences the outgassing measurement reproducibility.

Reproducibility is important for comparing the behaviour of different types of graphite.

Therefore, for future tests we consider it appropriate to use the known "conductance method", which should guarantee a better reproducibility of results.

Reference

/1/ "Inficon Quadrex 200" residual gas analyser technical manual. Theory and interpretation.

Figure captions

Fig. 1	Schematic of the outgassing facility
Fig. 2	Ionization gauge calibration
Fig. 3	Quadrupole dynamic calibration for H_2
Fig. 4	Quadrupole dynamic calibration for CH_4
Fig. 5	Quadrupole dynamic calibration for N_2
Fig. 6	Quadrupole dynamic calibration for Ar
Fig. 7	1st sample - quadrupole calibration
Fig. 8	2nd sample - quadrupole calibration
Fig. 9	1st sample - quadrupole current vs absolute press
Fig. 10	2nd sample - quadrupole current vs absolute press
Fig. 11	Chamber temp. vs sample temp.
Fig. 12	Background outgassing rate vs chamber temp.
Fig. 13	Background outgassing rate vs sample temp.
Fig. 14	sample No. 1 - outgassing rate
Fig. 15	sample No. 2 - outgassing rate

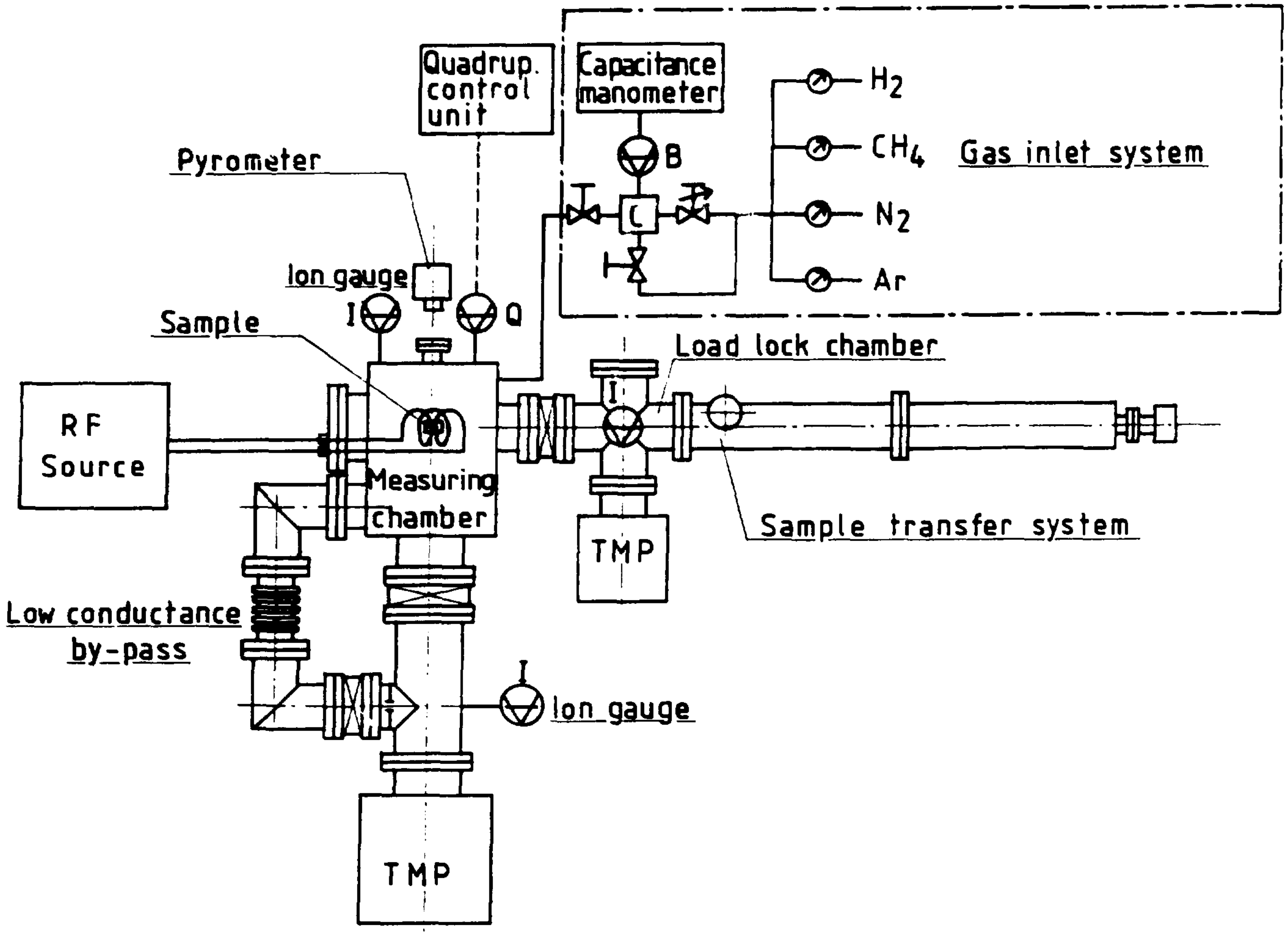

FIG.1 Schematic of the outgassing facility

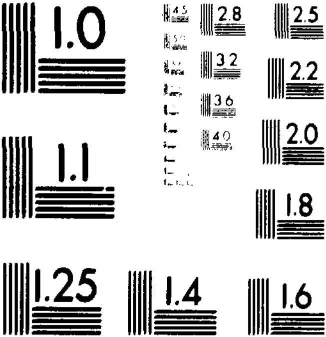

MICROCOPY RESOLUTION TEST CHART
NATIONAL BUREAU OF STANDARDS
STANDARD REFERENCE MATERIAL 1010a
(ANSI and ISO TEST CHART No. 2)

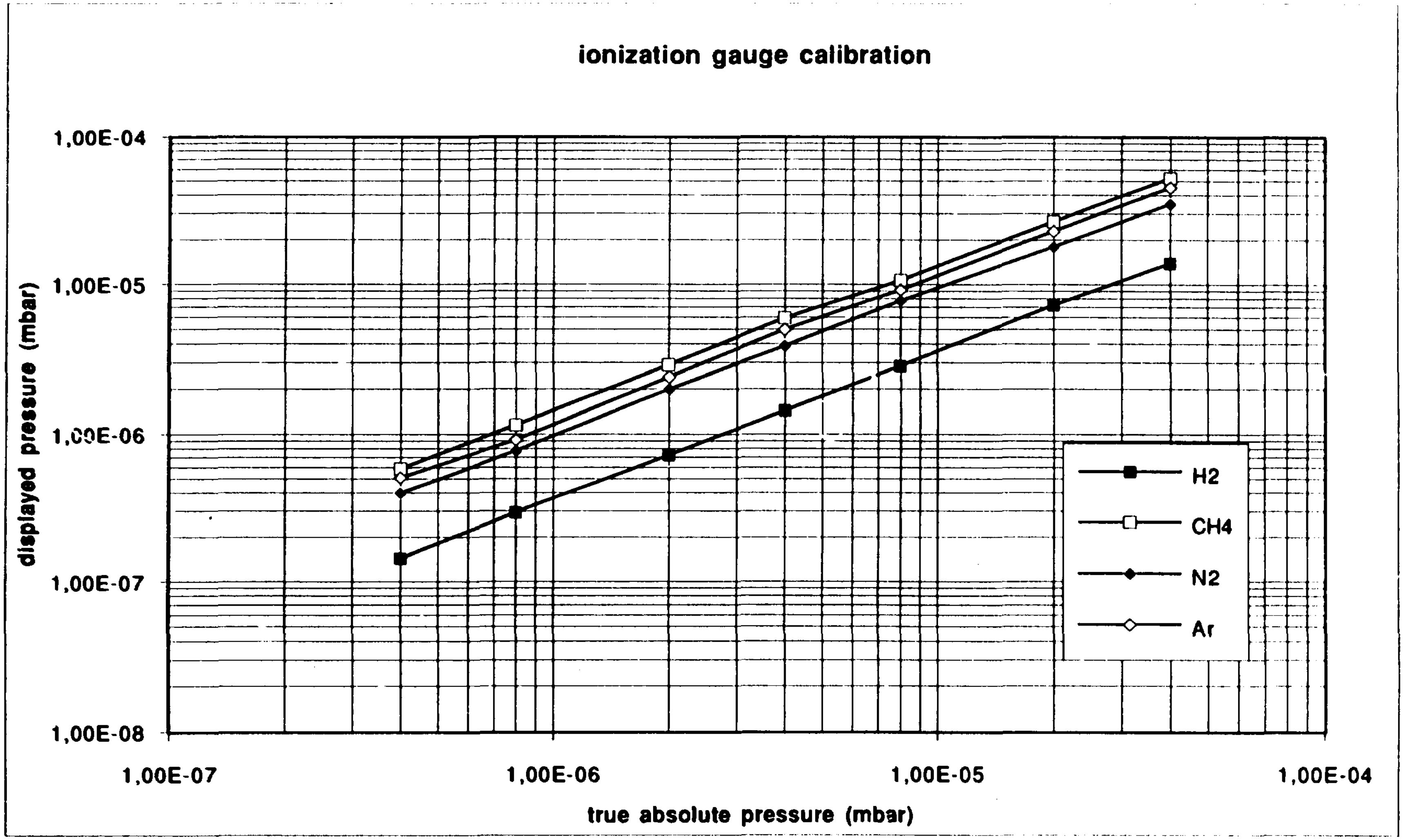
ionization gauge calibration
displayed pressure (mbar)
1,00E-04
1,00E-05
1,00E-06
1,00E-07
1,00E-08
true absolute pressure (mbar)
1,00E-07
1,00E-06
1,00E-05
1,00E-04
H2
CH4
N2
Ar

fig.2

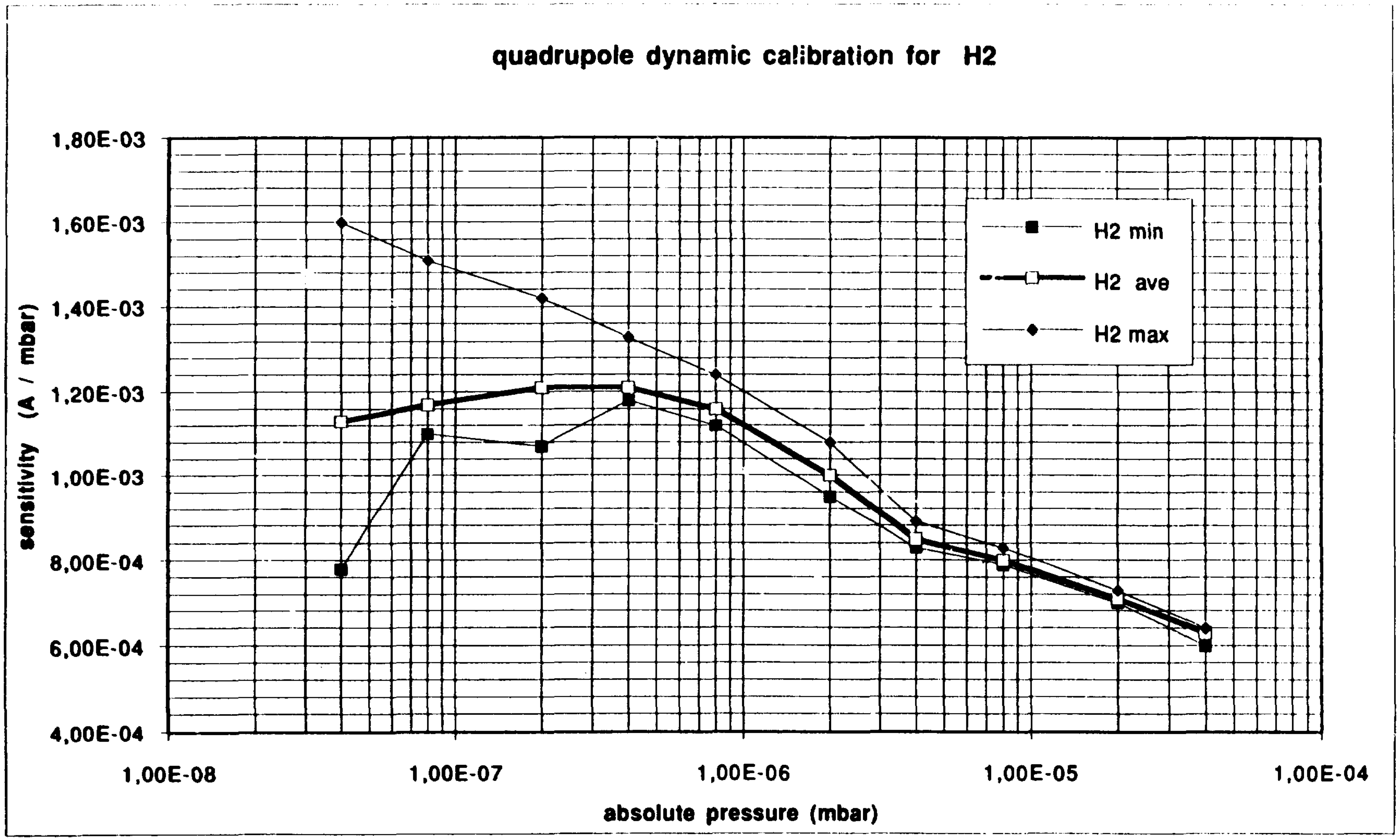
quadrupole dynamic calibration for H2
sensitivity (A / mbar)
1,80E-03
1,60E-03
1,40E-03
1,20E-03
1,00E-03
8,00E-04
6,00E-04
4,00E-04
1,00E-08
1,00E-07
1,00E-06
1,00E-05
1,00E-04
absolute pressure (mbar)
H2 min
H2 ave
H2 max

fig.3

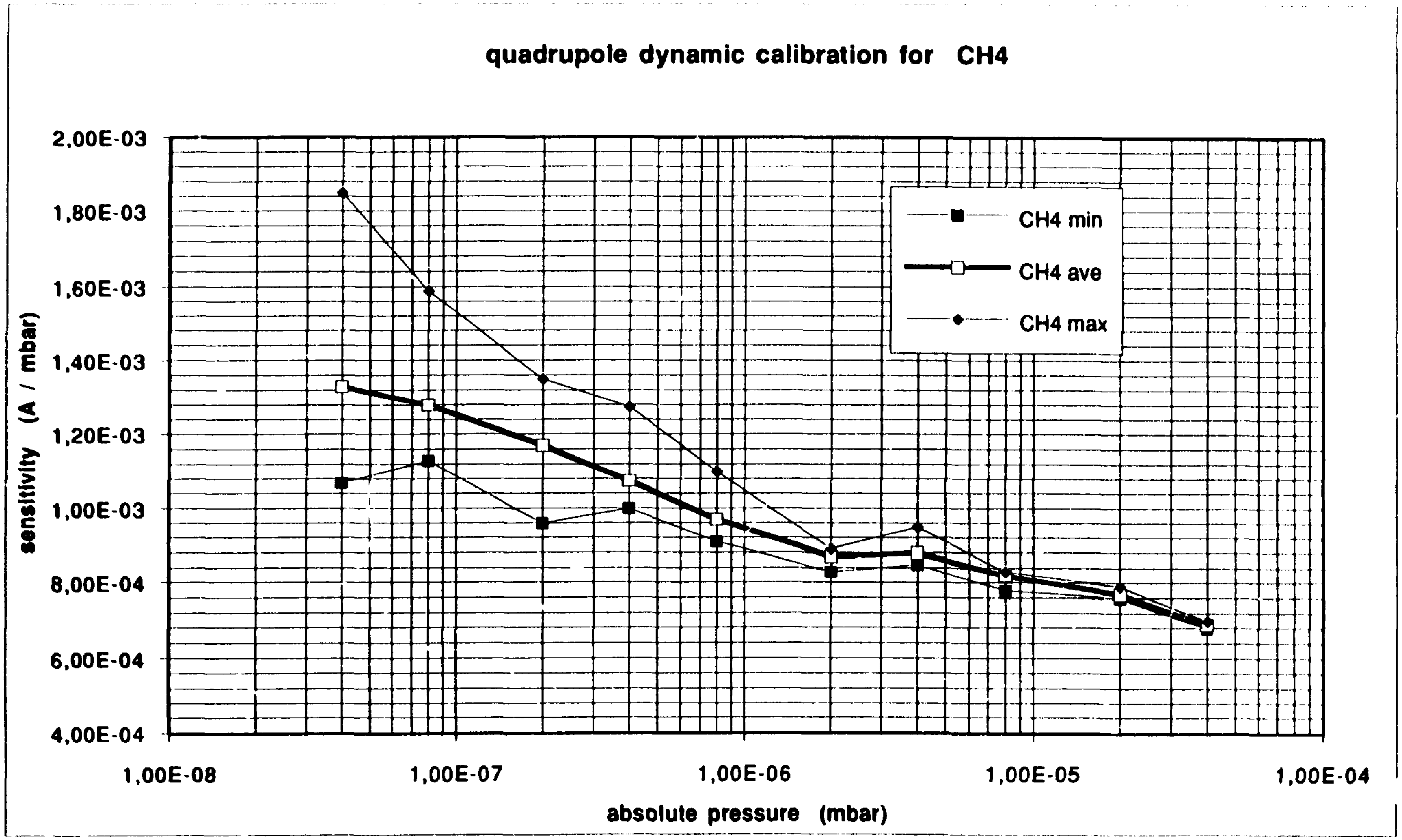

quadrupole dynamic calibration for CH4
2,00E-03
1,80E-03
1,60E-03
1,40E-03
1,20E-03
1,00E-03
8,00E-04
6,00E-04
4,00E-04
sensitivity (A / mbar)
1,00E-08
1,00E-07
1,00E-06
1,00E-05
1,00E-04
absolute pressure (mbar)
CH4 min
CH4 ave
CH4 max

fig.4

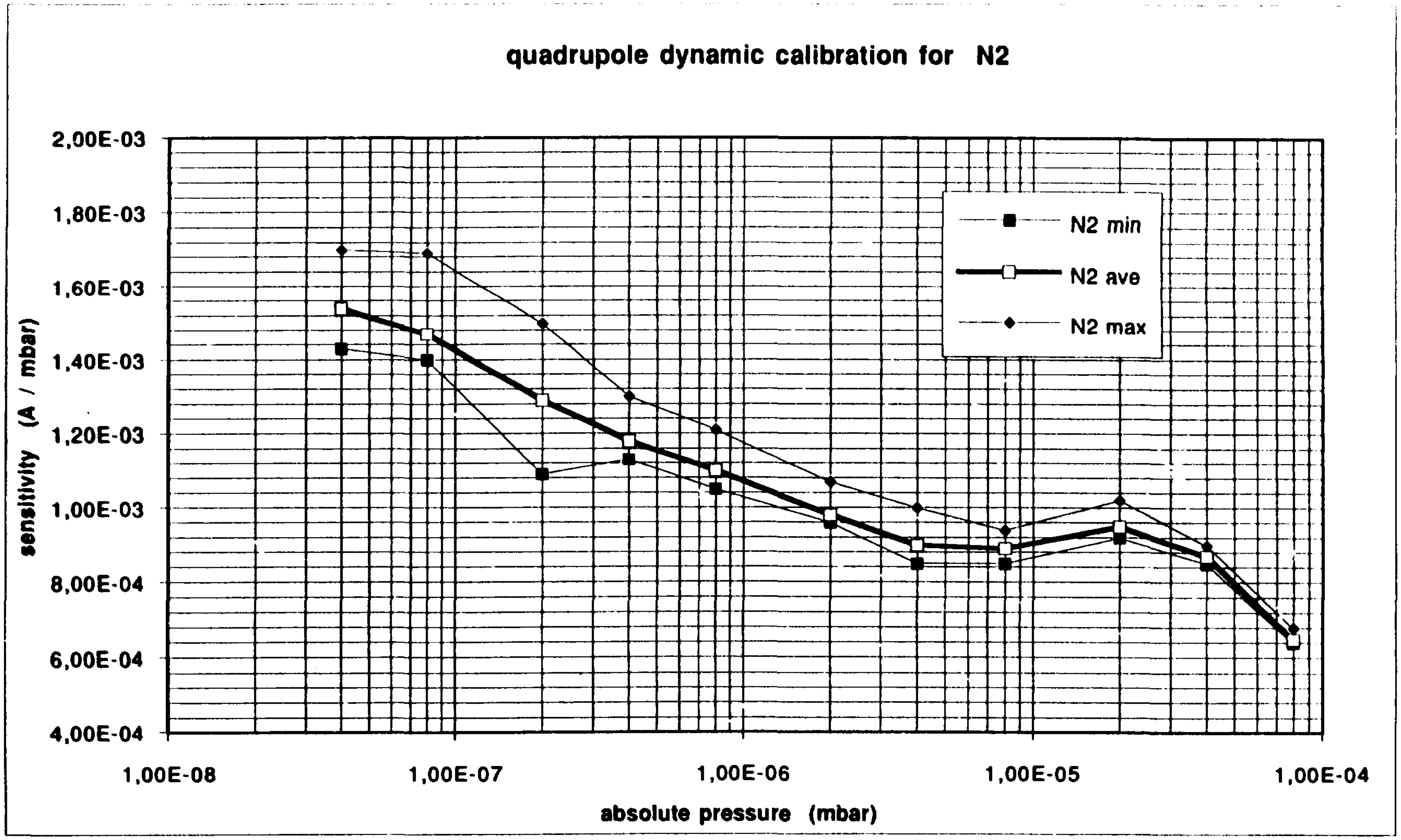
quadrupole dynamic calibration for N2
2,00E-03
1,80E-03
1,60E-03
1,40E-03
1,20E-03
1,00E-03
8,00E-04
6,00E-04
4,00E-04
sensitivity (A / mbar)
1,00E-08
1,00E-07
1,00E-06
1,00E-05
1,00E-04
absolute pressure (mbar)
N2 min
N2 ave
N2 max

fig.5

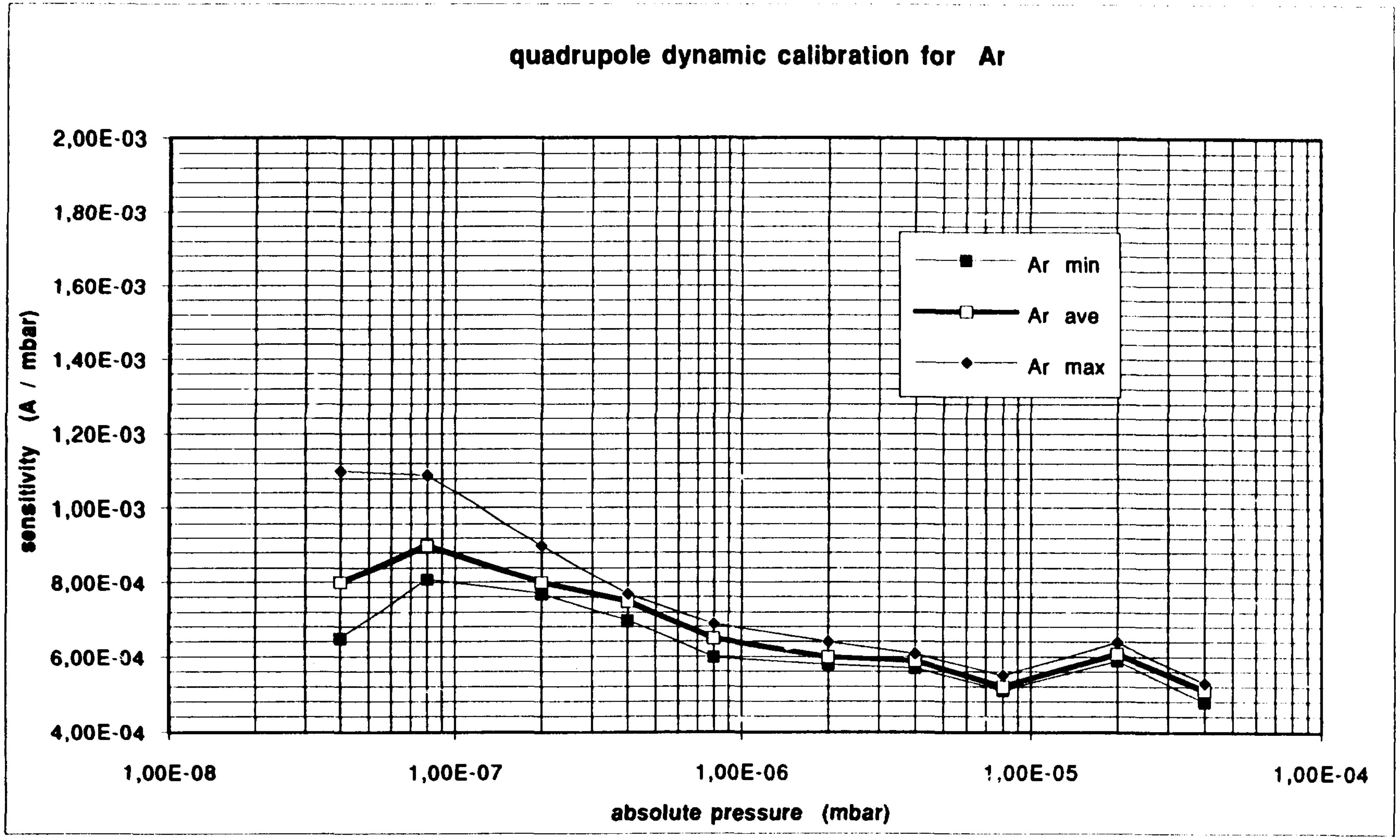
quadrupole dynamic calibration for Ar
sensitivity (A / mbar)
2,00E-03
1,80E-03
1,60E-03
1,40E-03
1,20E-03
1,00E-03
8,00E-04
6,00E-04
4,00E-04
1,00E-08
1,00E-07
1,00E-06
1,00E-05
1,00E-04
absolute pressure (mbar)
Ar min
Ar ave
Ar max

fig.6

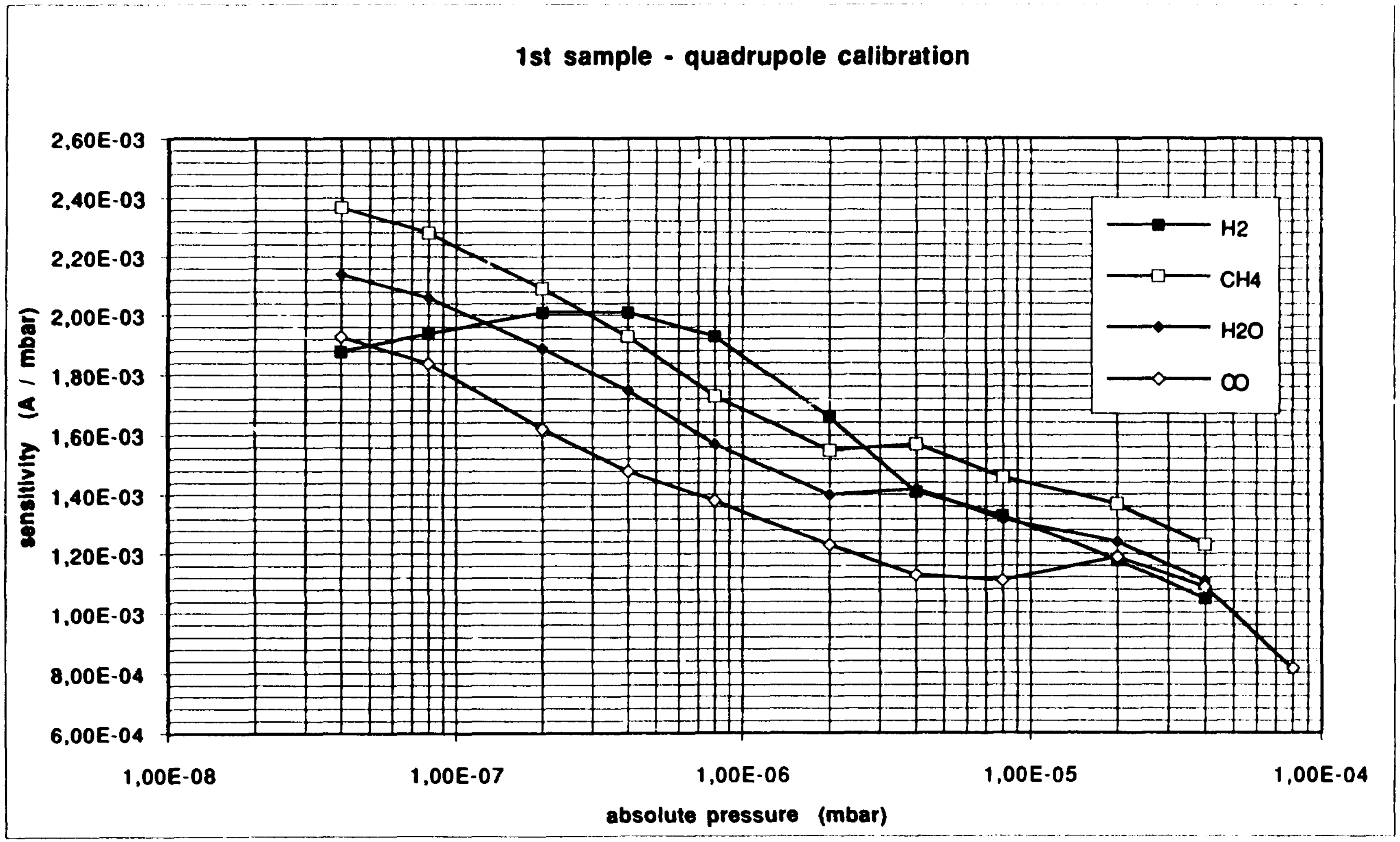
1st sample - quadrupole calibration
sensitivity (A / mbar)
2,60E-03
2,40E-03
2,20E-03
2,00E-03
1,80E-03
1,60E-03
1,40E-03
1,20E-03
1,00E-03
8,00E-04
6,00E-04
1,00E-08
1,00E-07
1,00E-06
1,00E-05
1,00E-04
absolute pressure (mbar)
H2
CH4
H2O
CO

fig 7

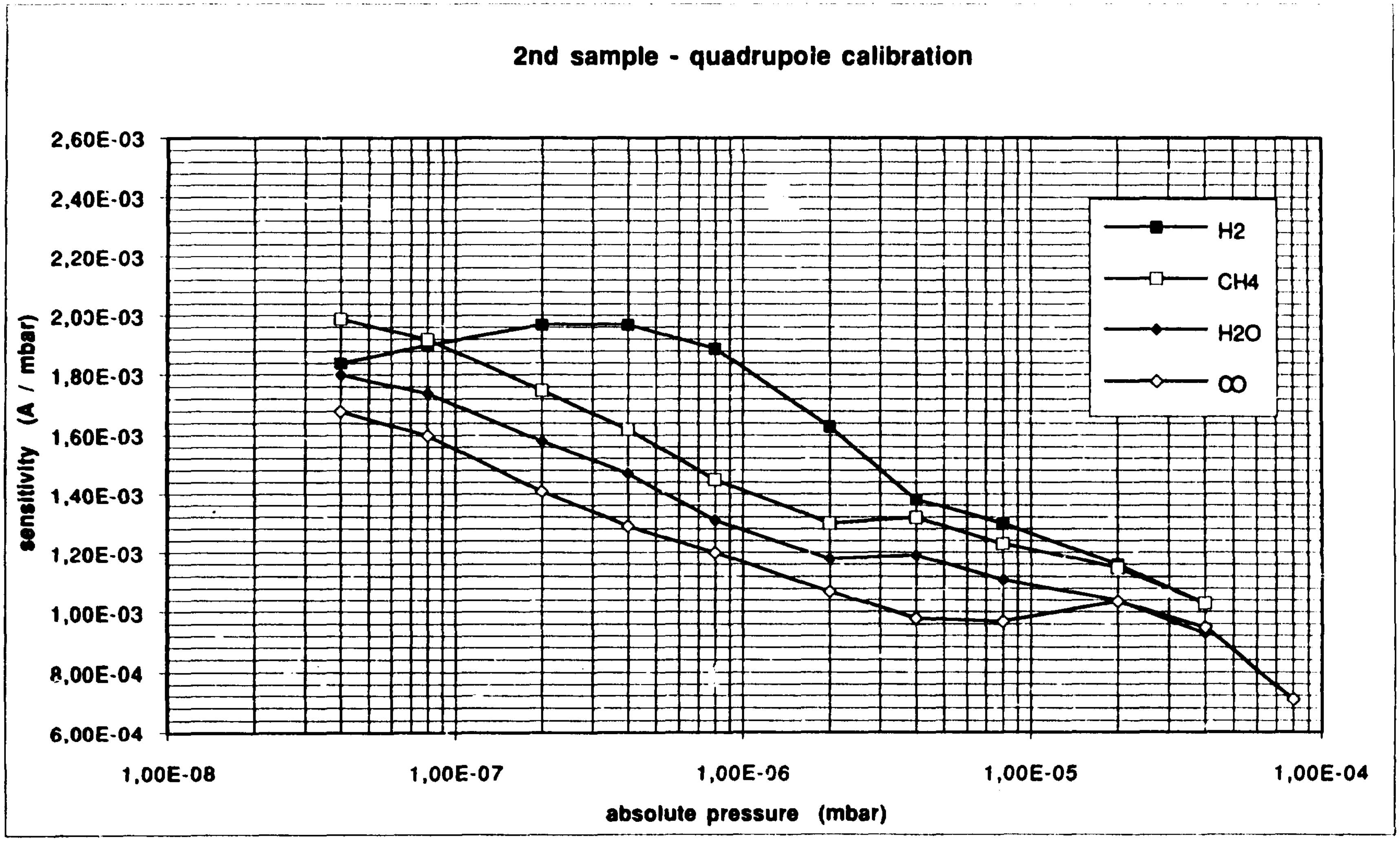
2nd sample - quadrupole calibration

fig.8

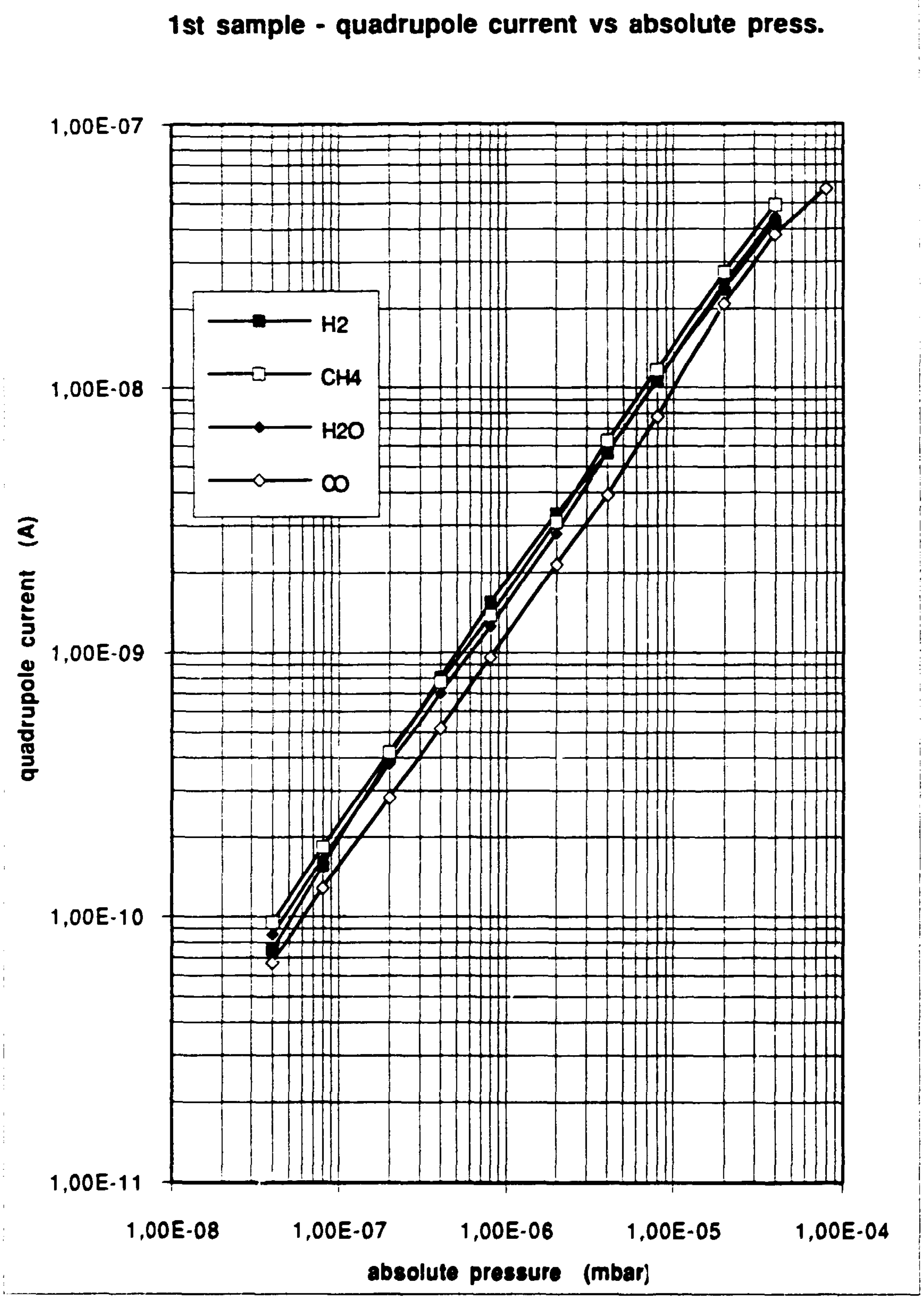
1st sample - quadrupole current vs absolute press.
1,00E-07
1,00E-08
1,00E-09
1,00E-10
1,00E-11
quadrupole current (A)
1,00E-08
1,00E-07
1,00E-06
1,00E-05
1,00E-04
absolute pressure (mbar)
H2
CH4
H2O
CO

fig.9

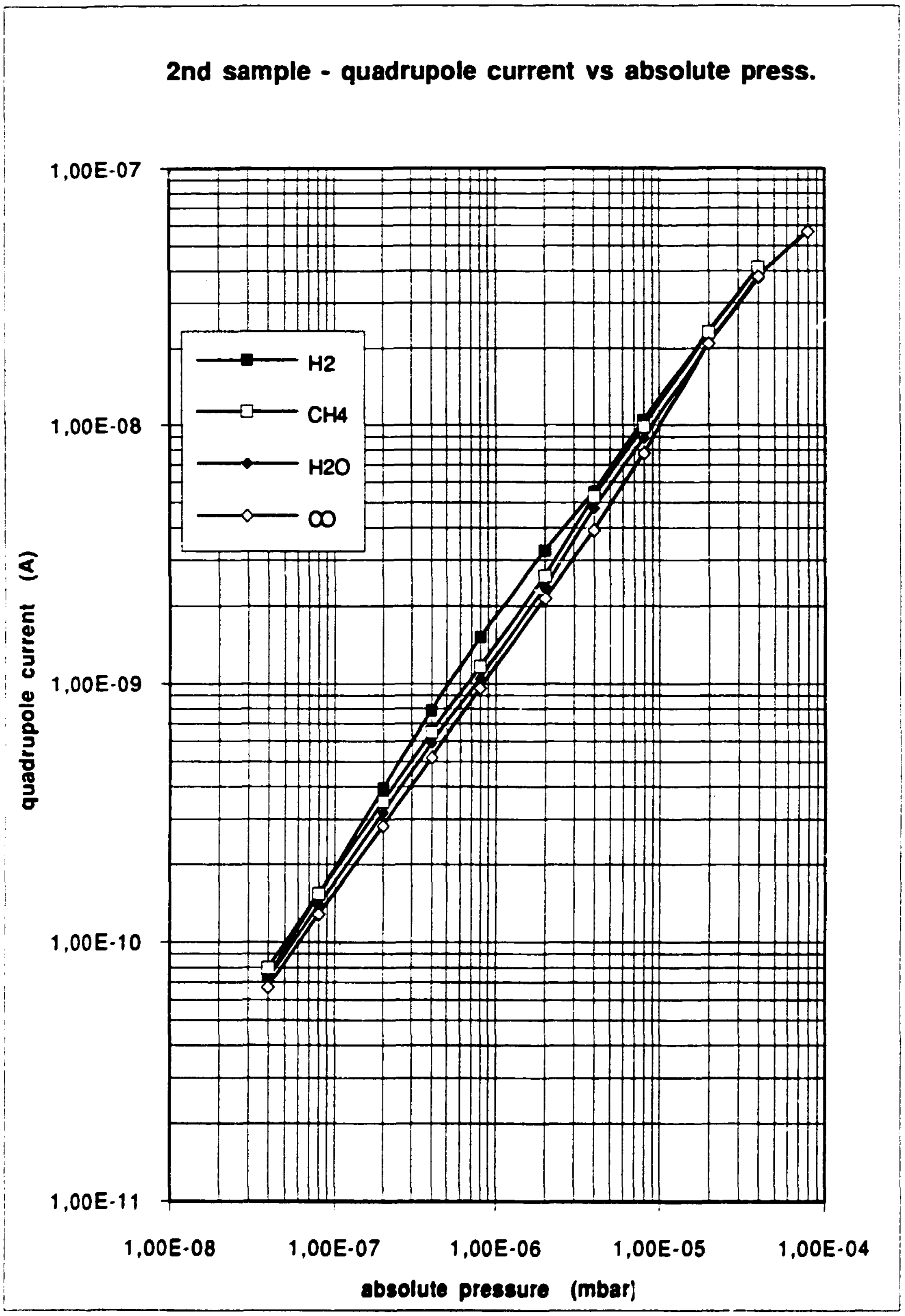
2nd sample - quadrupole current vs absolute press.
1,00E-07
1,00E-08
1,00E-09
1,00E-10
1,00E-11
quadrupole current (A)
1,00E-08
1,00E-07
1,00E-06
1,00E-05
1,00E-04
absolute pressure (mbar)
H2
CH4
H2O
CO

fig.10

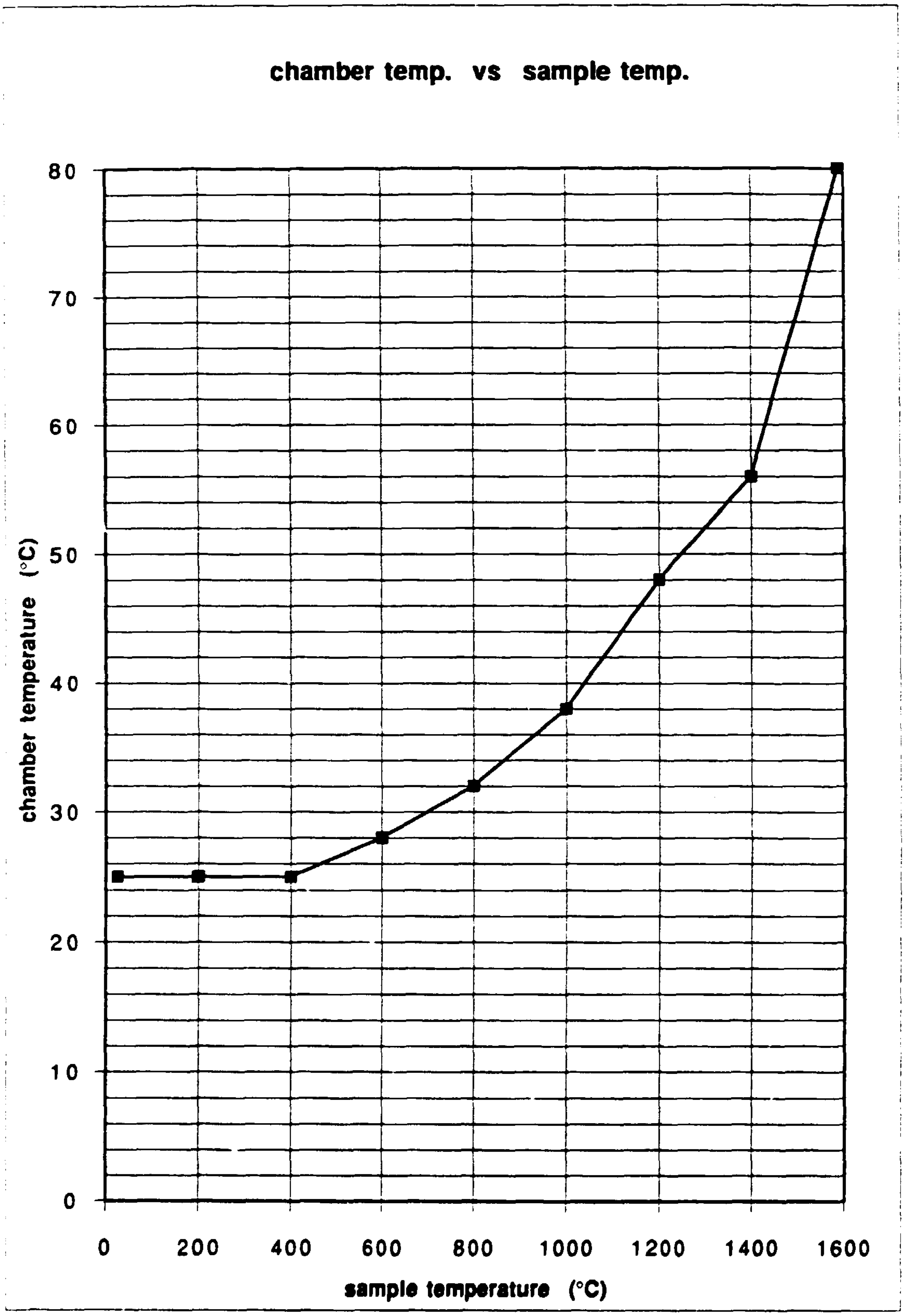
chamber temp. vs sample temp.
chamber temperature (°C)
80
70
60
50
40
30
20
10
0
0
200
400
600
800
1000
1200
1400
1600
sample temperature (°C)

fig.11

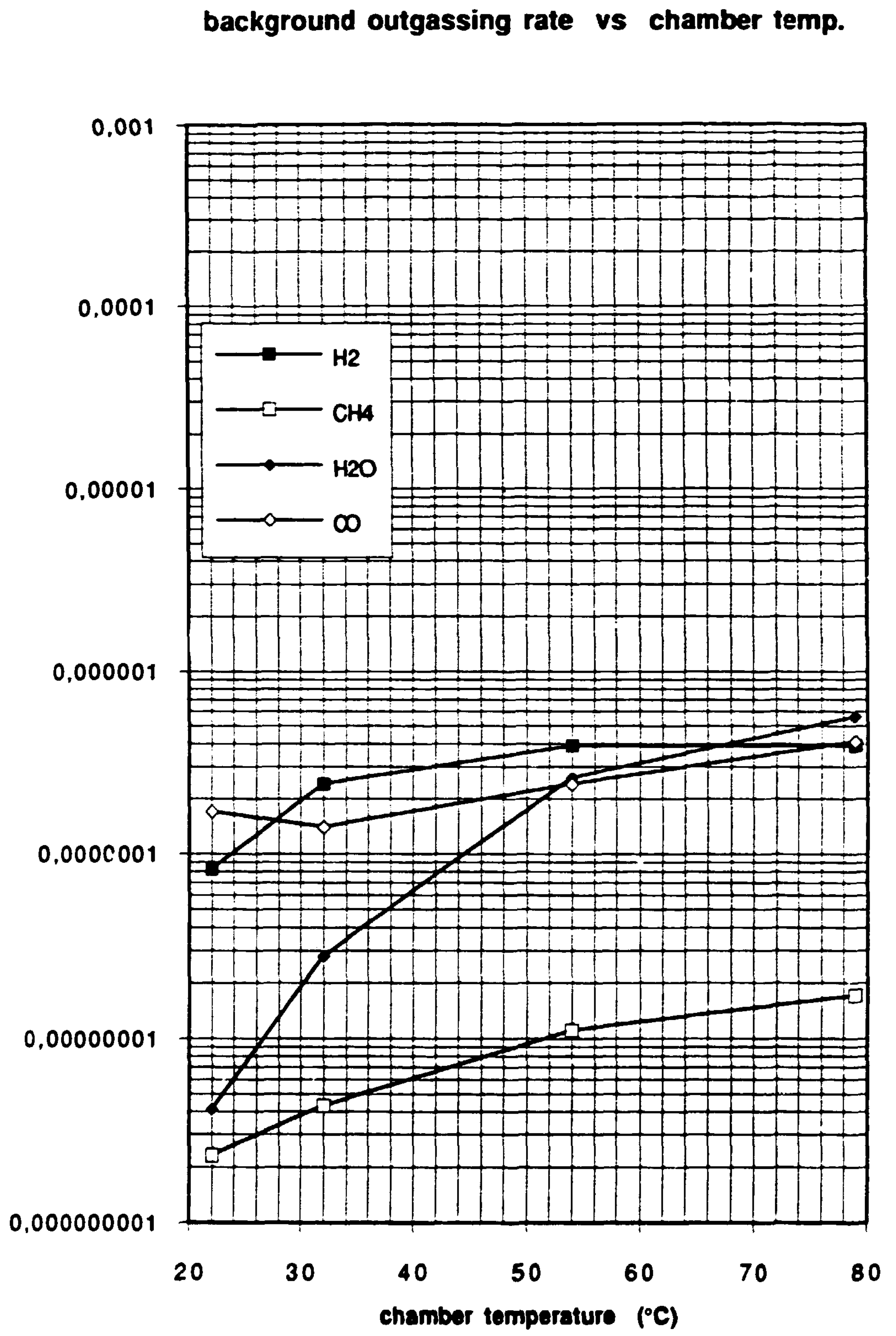

background outgassing rate vs chamber temp.
0,001
0,0001
0,00001
0,000001
0,0000001
0,00000001
0,000000001
mbar l / s
H2
CH4
H2O
CO
20
30
40
50
60
70
80
chamber temperature (°C)

fig.12

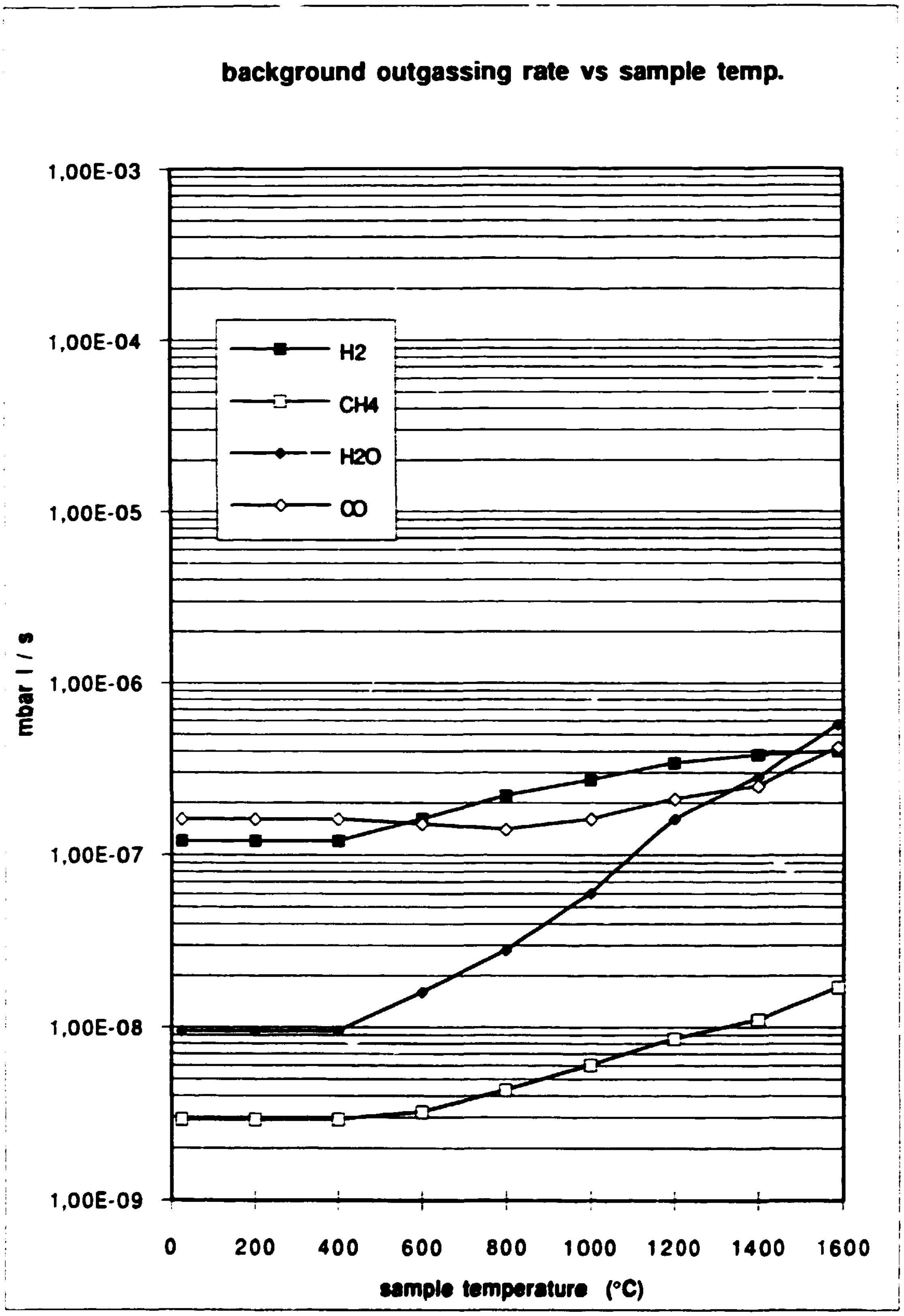
background outgassing rate vs sample temp.
1,00E-03
1,00E-04
1,00E-05
1,00E-06
1,00E-07
1,00E-08
1,00E-09
mbar l / s
H2
CH4
H2O
CO
0
200
400
600
800
1000
1200
1400
1600
sample temperature (°C)

fig.13

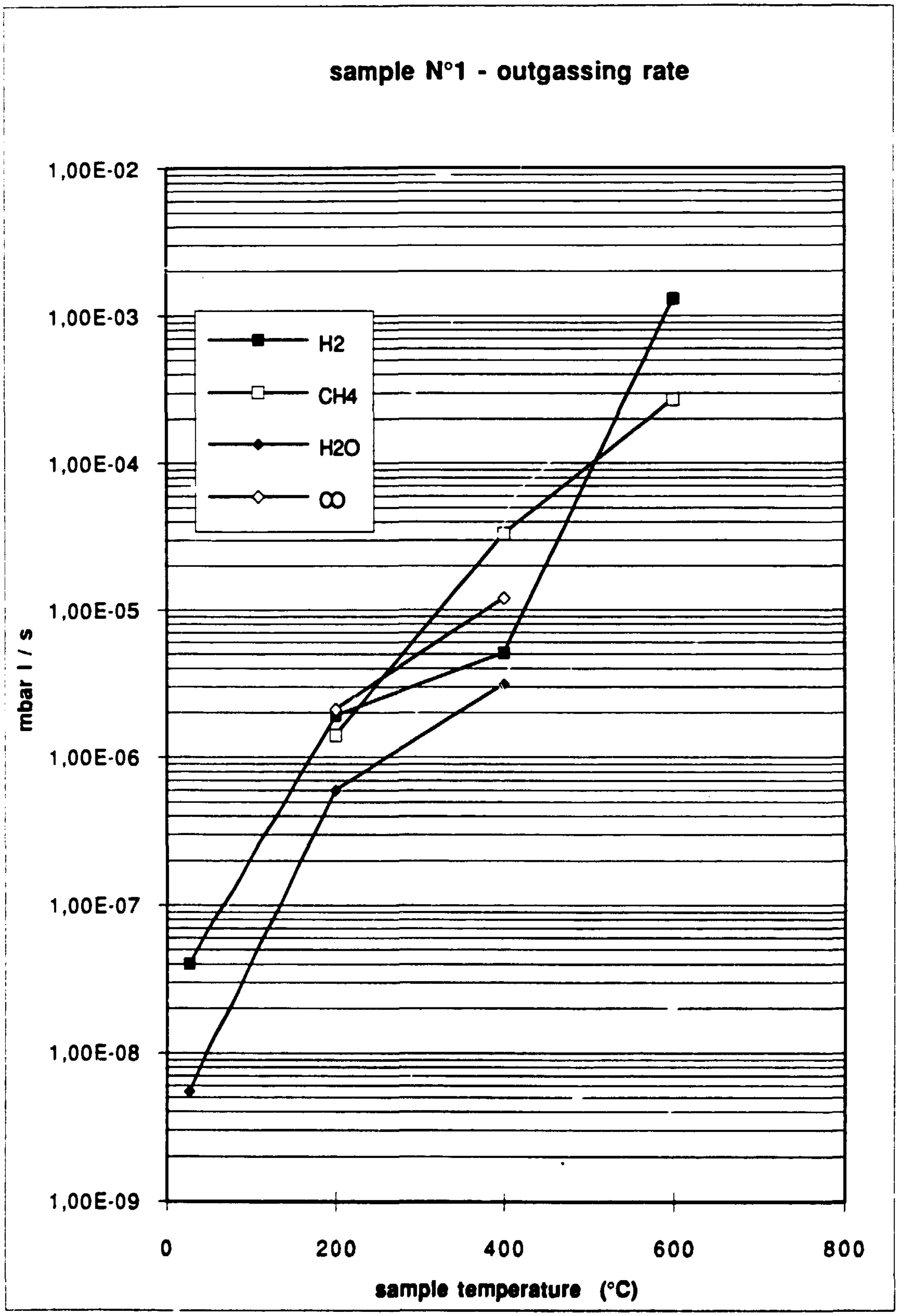
sample N°1 - outgassing rate
1,00E-02
1,00E-03
1,00E-04
1,00E-05
1,00E-06
1,00E-07
1,00E-08
1,00E-09
mbar l / s
H2
CH4
H2O
CO
0
200
400
600
800
sample temperature (°C)

fig.14

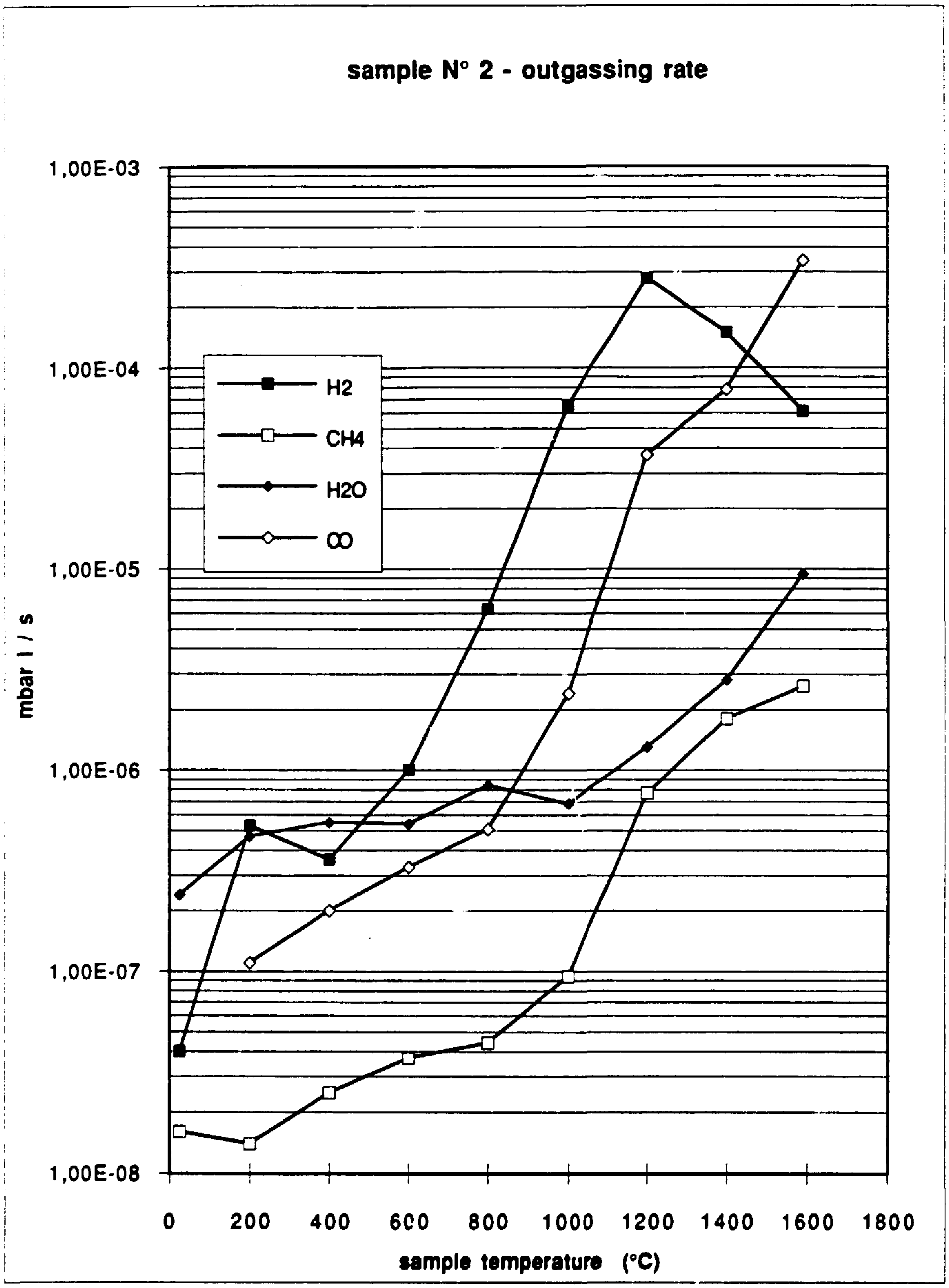

sample N° 2 - outgassing rate
1,00E-03
1,00E-04
1,00E-05
1,00E-06
1,00E-07
1,00E-08
mbar l / s
H2
CH4
H2O
CO
0
200
400
600
800
1000
1200
1400
1600
1800
sample temperature (°C)

fig.15